Static and Fatigue Failure of Bolted Joints in Hybrid Composite-Aluminium Aircraft Structures

Zlatan Kapidzic
SAAB Aeronautics
Sweden

Hybrid structures

- Aluminium Alloys (AA)
- Carbon-Fibre Composite (CFRP)
- Glass-Fibre Composite (GFRP)
- Aramid-Fibre Composite (AFRP)

➢ Structures composed of two or more materials.

➢ Distinct interface where the materials are joined, commonly by bolted joints.

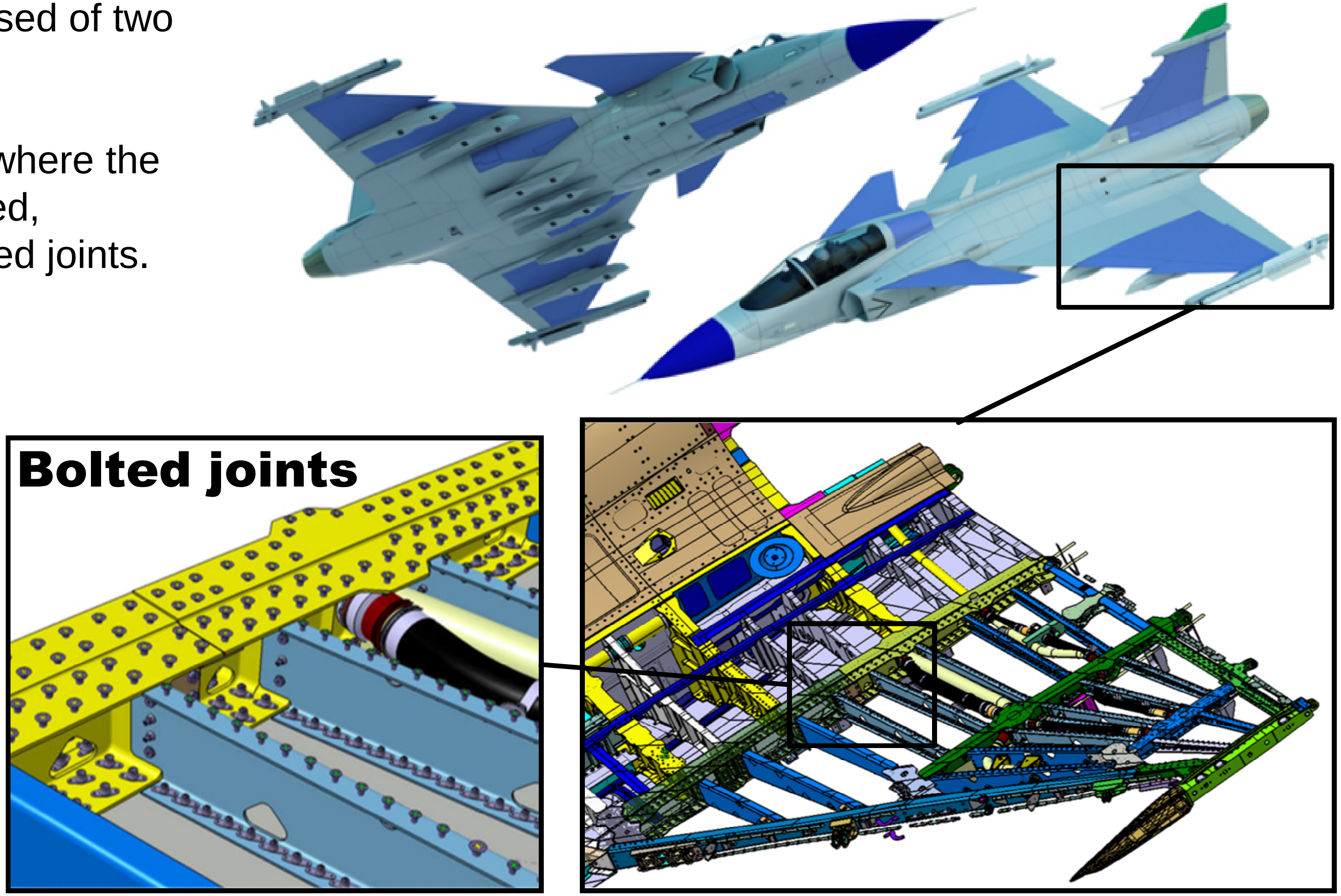

CFRP-AA hybrid structures

Significant differences between CFRP and AA:

- Thermal expansion properties
  $\alpha_{CFRP} = 2.1 \cdot 10^{-6}\ {}^{o}C^{-1}$,
  $\alpha_{AA} = 23.4 \cdot 10^{-6}\ {}^{o}C^{-1}$
- Failure mechanisms
- Sensitivity to loading type
  (tensile, compressive, out-of-plane)
- Statistical variability
- Defect resistance
- Anisotropy
- Density
- Environmental sensitivity
- Design and airworthiness requirements

Etc.

Hybrid

Structural issues:

- Thermally induced loads
- Difficult to predict structural failure modes
- Buckling and permanent deformations
- Testing (accounting for scatter, significant load states and levels)
- Design and analysis methods

Etc.

Structural integrity assessment

- Aims to ensure airworthiness, structural integrity and durability.

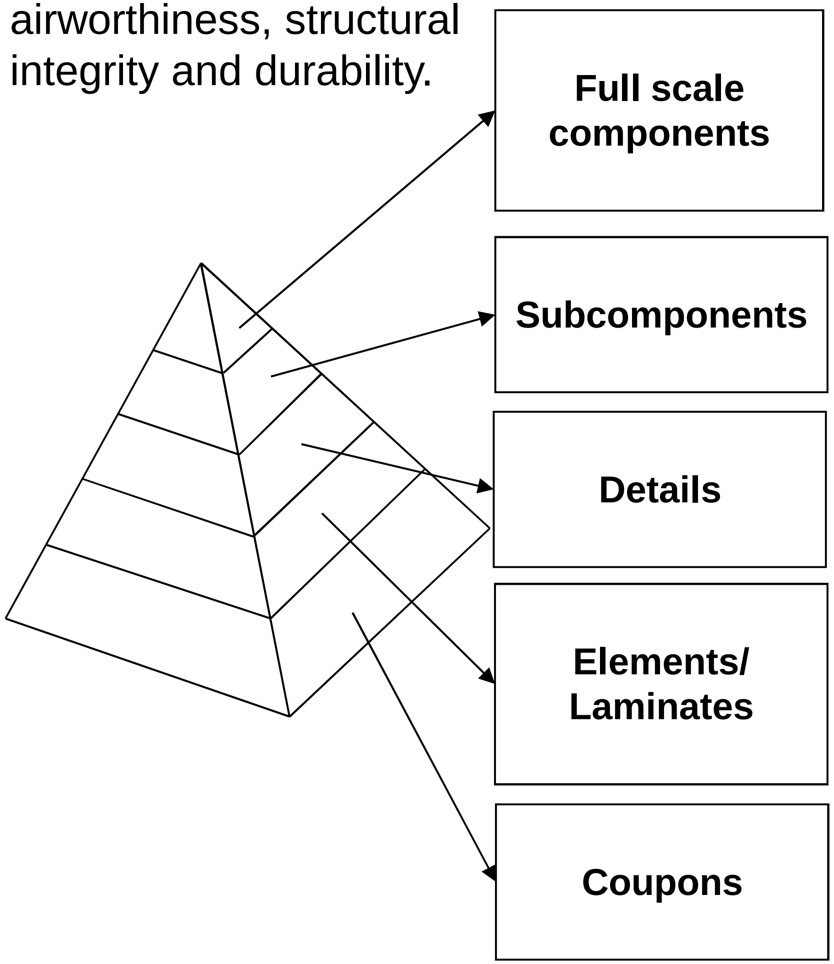

TESTING

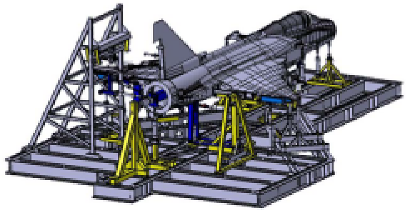

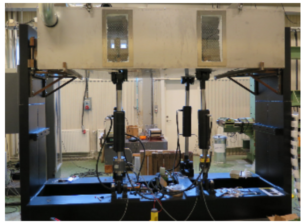

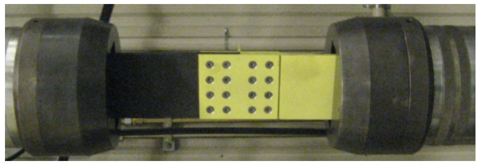

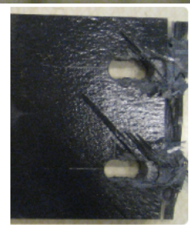

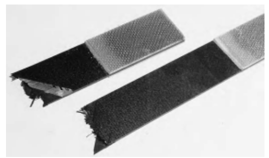

ANALYSIS

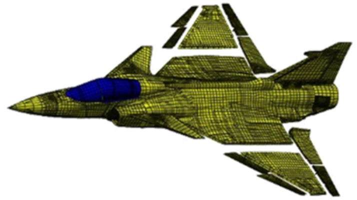

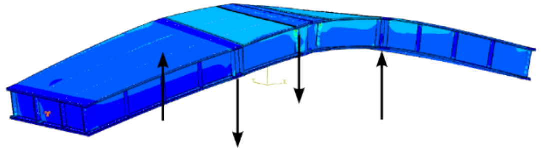

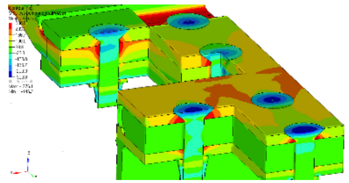

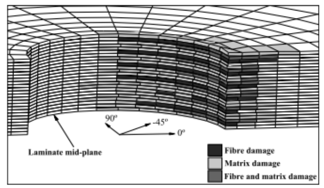

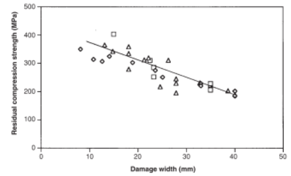

NFFP6 Effect of thermally induced bolt load on the bearing strength of CFRP

- At elevated temperature, hybrid CFRP/AA structures develop thermally induced loads due to $\alpha_{CFRP} << \alpha_{AA}$.
- In bolted joints, this leads to a biaxial bearing load state, $\mathbf{F} + \mathbf{F_{th}}$.

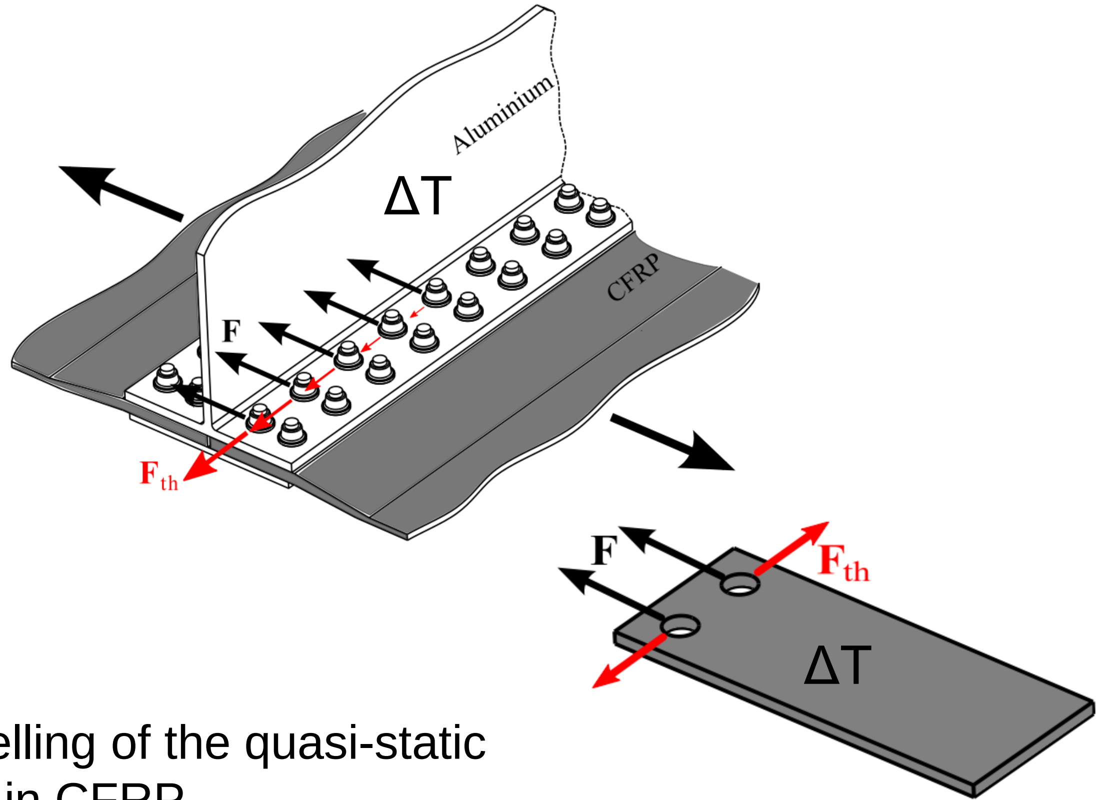

Research goals:

- Characterization and modelling of the quasi-static and fatigue bearing failure in CFRP.
- Influence of $\mathbf{F_{th}}$ on the static and fatigue bearing failure in CFRP.

Biaxial testing at elevated temperature

- Test rig, where a mechanical load, **F**, and a constant thermally induced load, **F_{th}**, were applied by mechanical actuators.
- Two-bolt, quasi-isotropic CFRP specimens.
- Uniaxial and biaxial static and fatigue tests at 90°C.

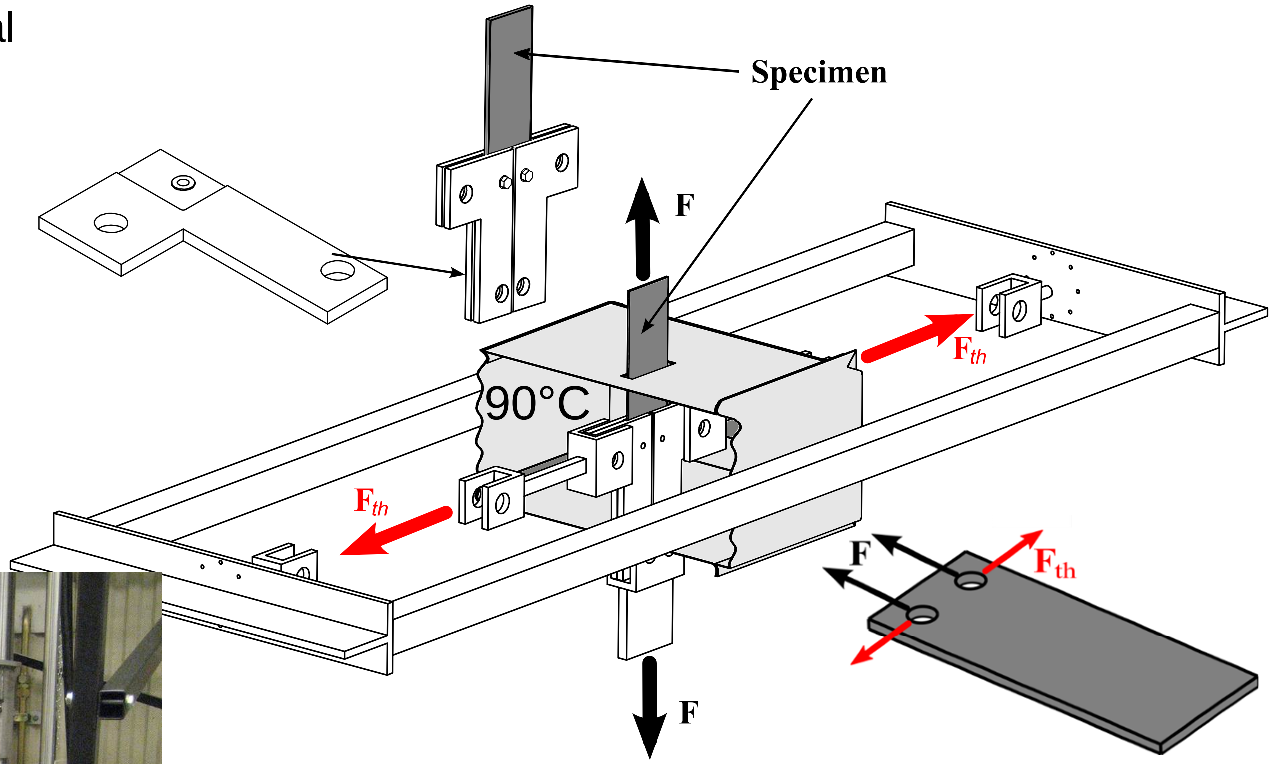

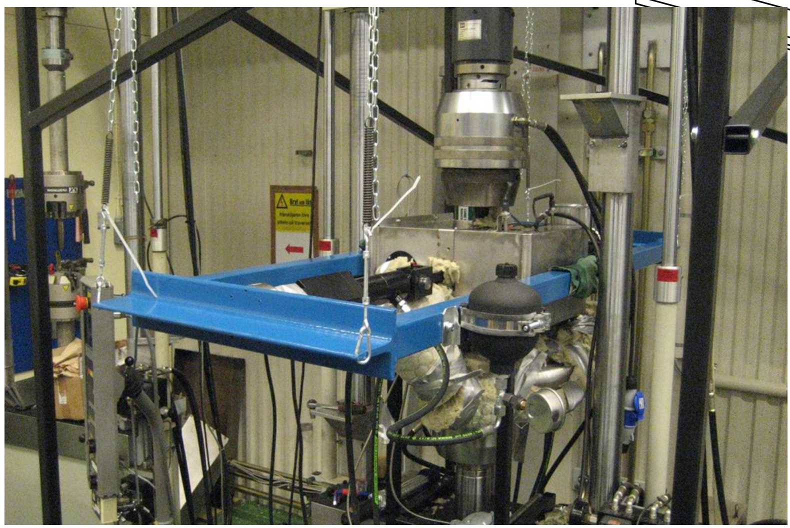

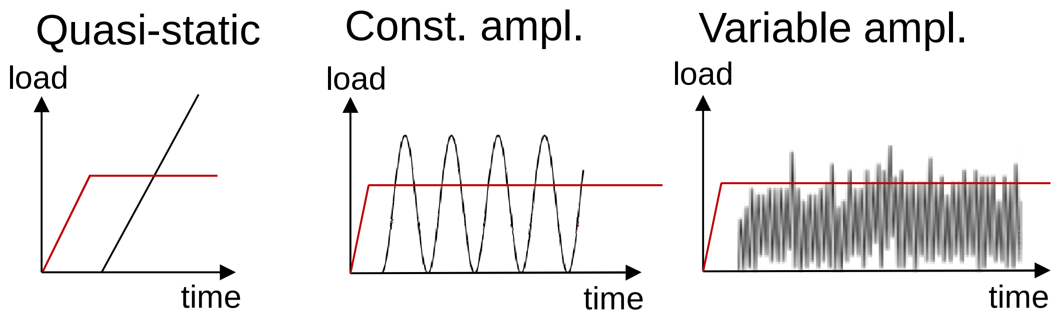

Observed failure mechanisms in static tests

- Fractography of the bearing plane of specimens loaded to 90% of the static failure load.
- Main failure mechanisms fiber kinking and matrix cracking, contained in shear bands.
- Delaminations and micro-cracking also observed.

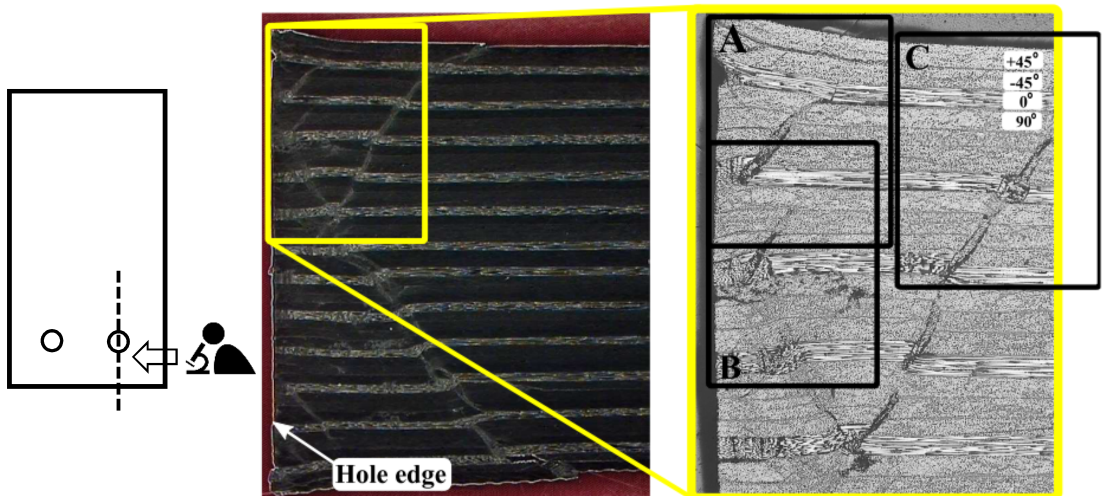

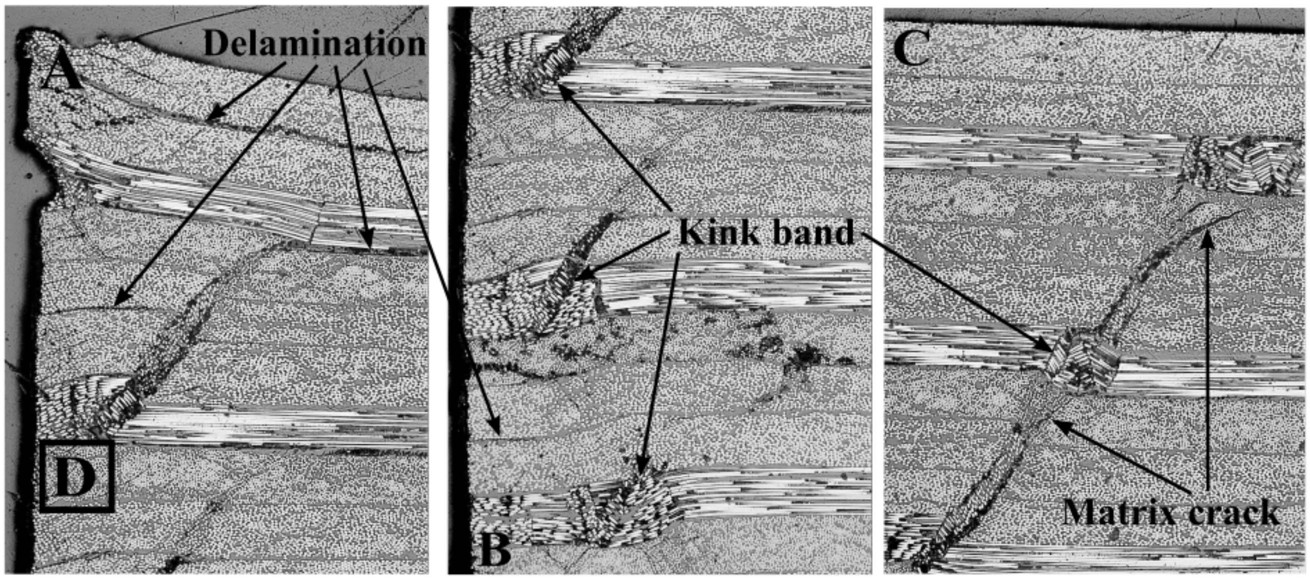

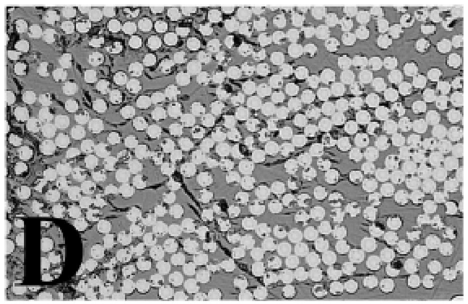

FE-modelling of static bearing failure

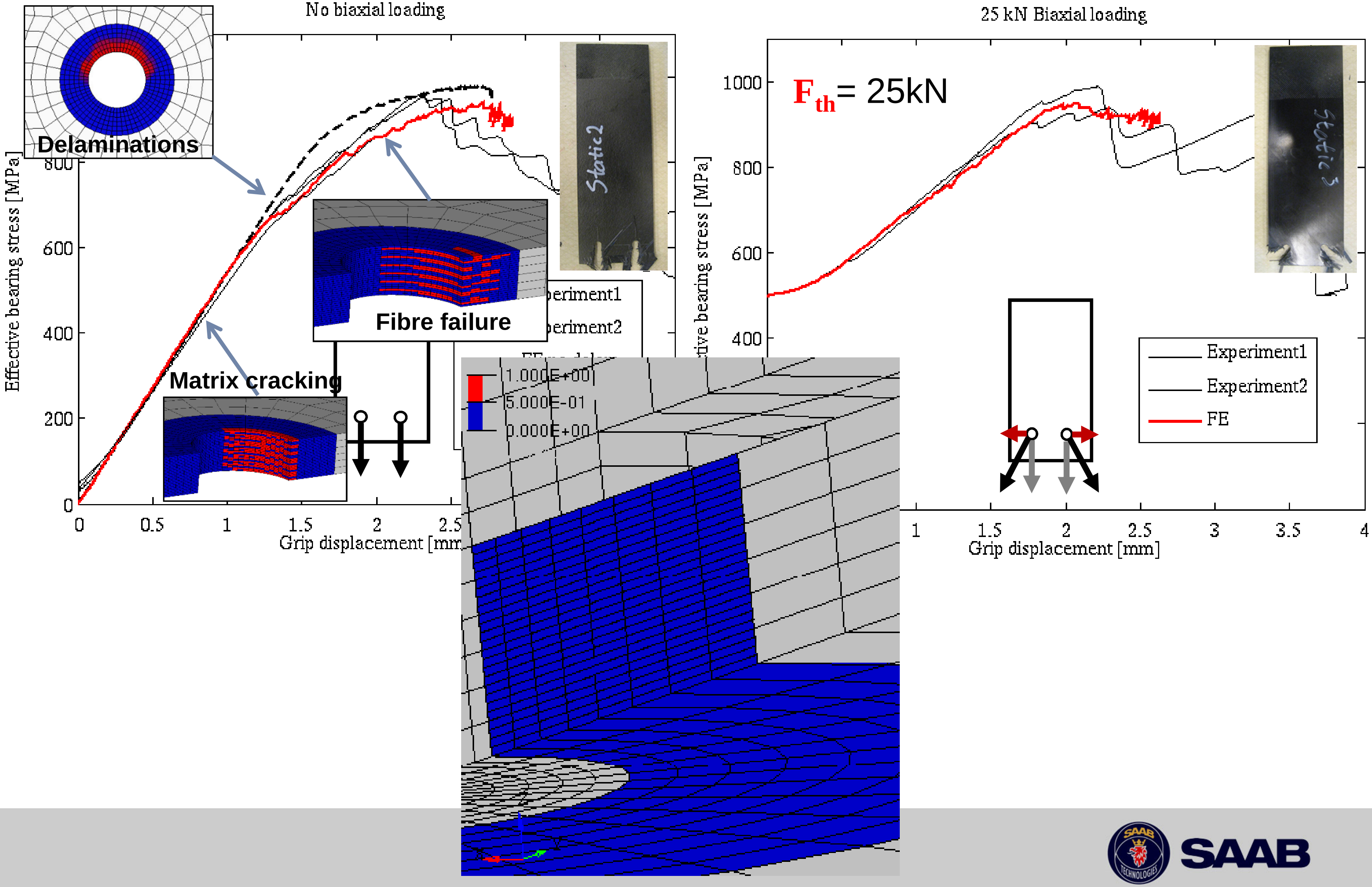

FE-modelling of static bearing failure in structure

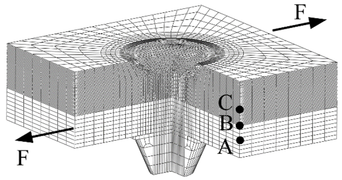

Local model

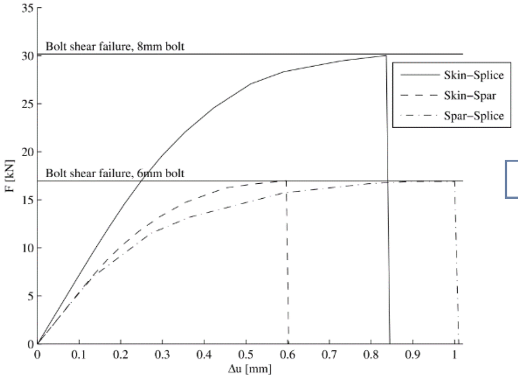

F-u response

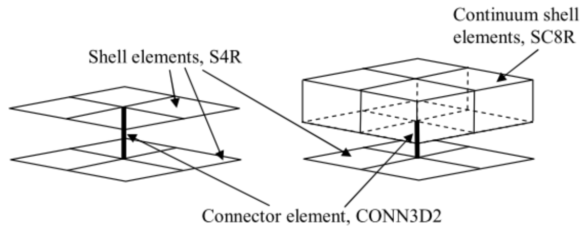

F-u response assigned to structural elements

Bolt load distribution

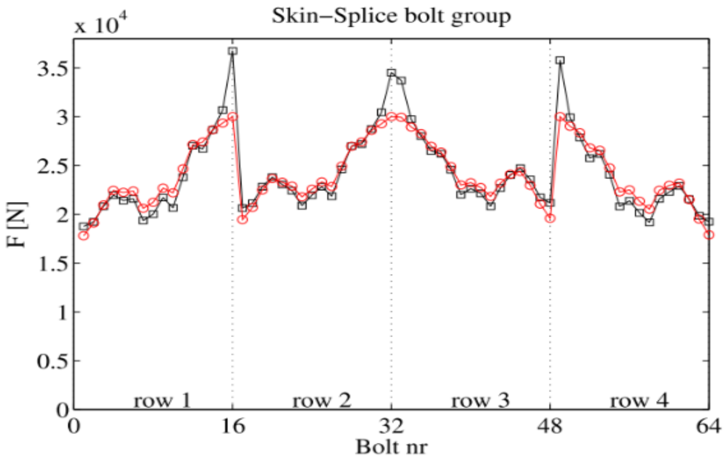

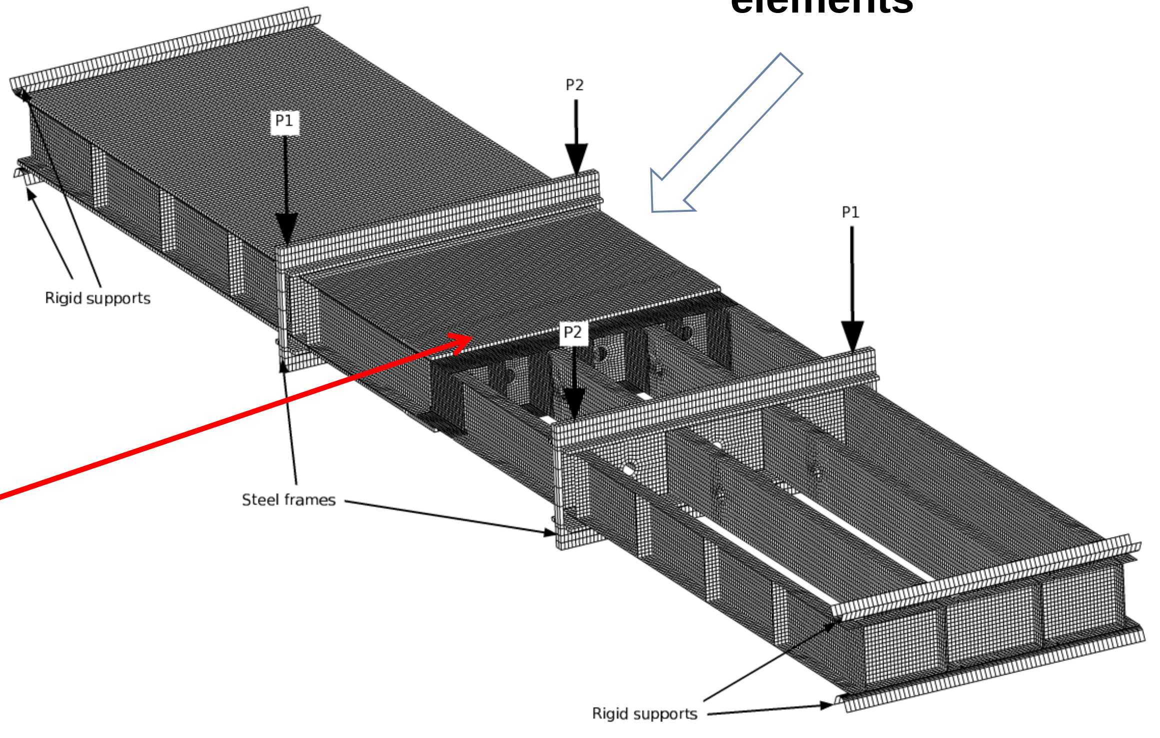

Observed failure mechanisms in fatigue tests

- Fractography at half-life shows that ply fracture is preceded by extensive micro-cracking of the matrix and of the fiber-matrix interfaces.

- Continuous out-of-plane bending of the plies is observed.

- Fatigue failure differs from static failure.

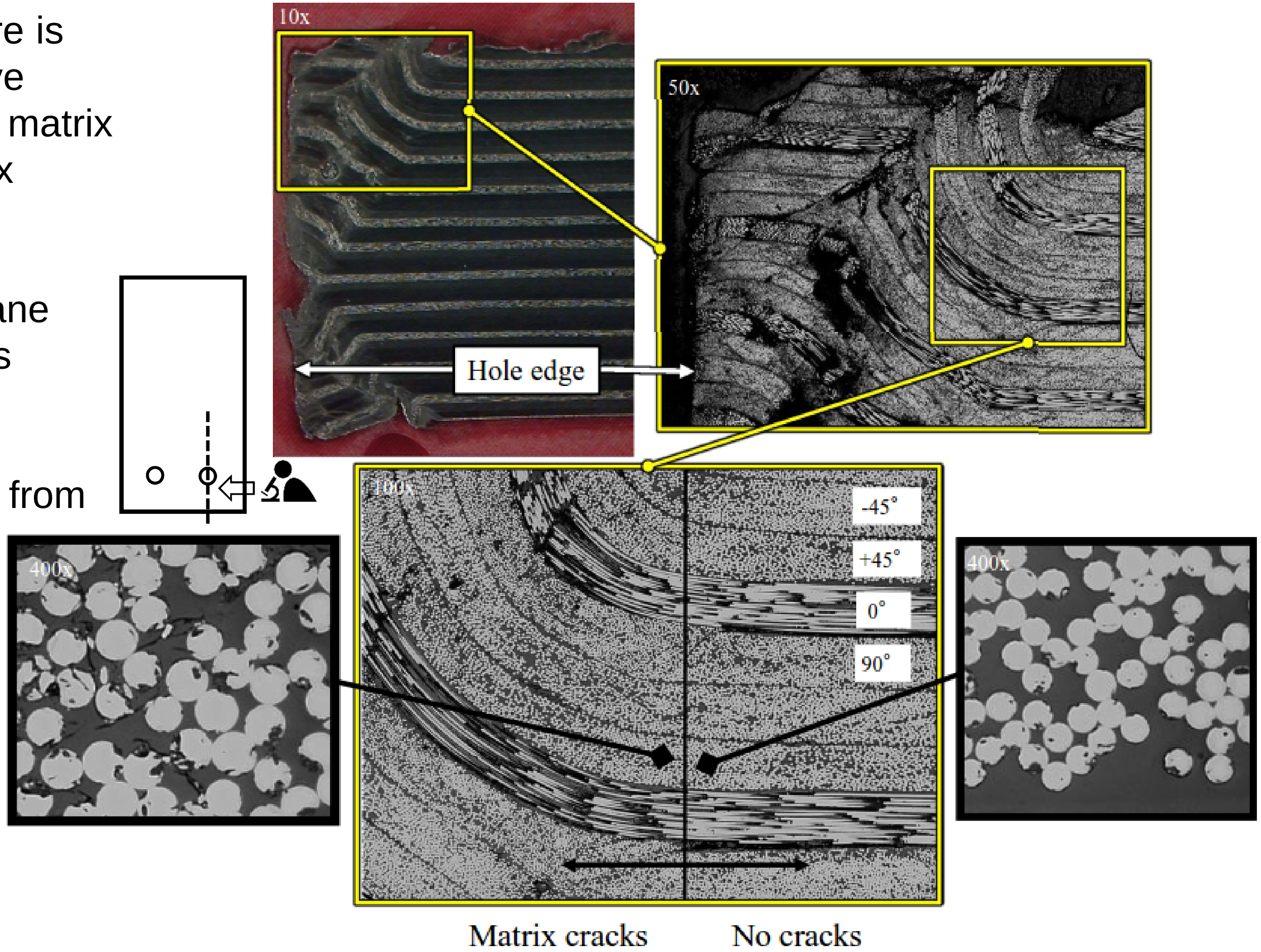

Observed failure behavior in fatigue tests

- Considerable softening of the laminate and hole elongation are observed continuously during the cycling in both constant and variable amplitude loading.

- The fatigue damage is generated during the whole process and not at a specific point in time, which is consistent with matrix micro-cracking.

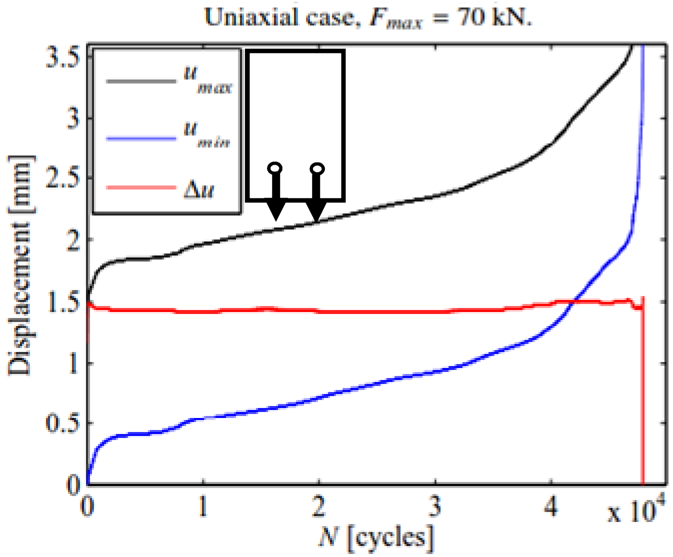

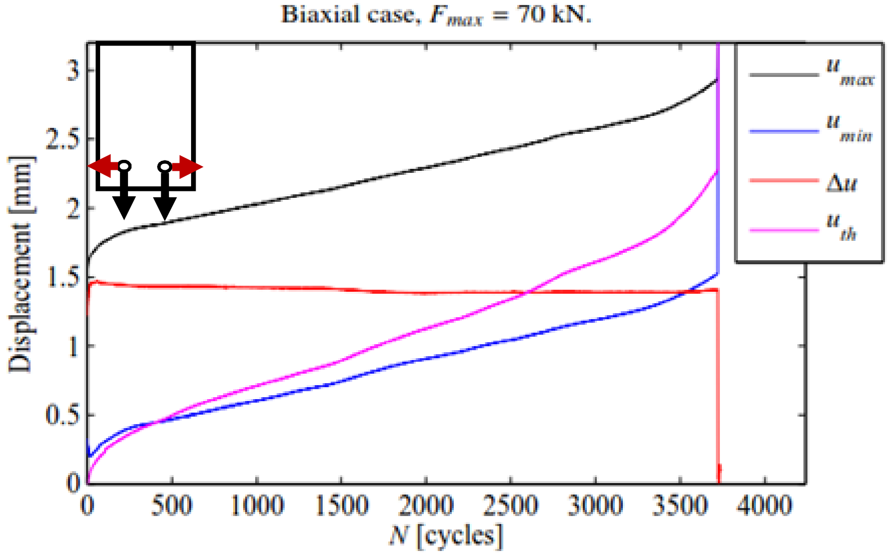

Fatigue failure modelling

- Based on kinetic theory of fracture for polymers and matrix micro-cracking.
- FE analysis and multi-continuum theory are used to compute the matrix stresses, on which the failure criterion is based.
- Temperature and loading frequency on the fatigue life are included in the model.

Parameter fitting, un-notched specimens

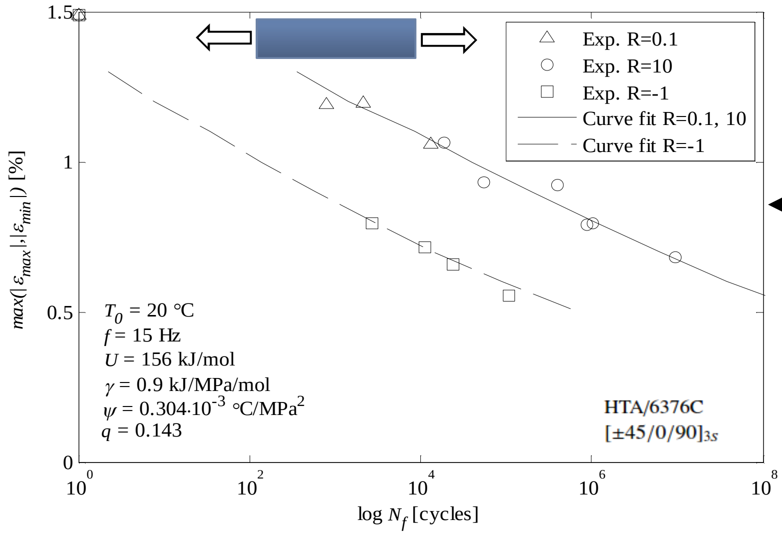

Homogenized ply properties

2D-FE

Average ply stress $\boldsymbol{\sigma}_c$

Homogenized fibre/matrix properties

MCT
(Multi-continuum theory)

Average matrix stress $\boldsymbol{\sigma}_{m,}$ σ

Kinetic theory of polymer fracture

$$\frac{dn}{dt} = (n_T - n)\frac{kT}{h}\exp\left(-\frac{U - \gamma\sigma(t)}{kT}\right)$$

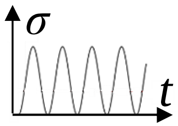

$$N_f = \frac{\frac{h}{kT}\exp\left(\frac{U}{kT}\right)}{\int_0^{1/f}\exp\left(\frac{\gamma\sigma(\tau)}{kT}\right)d\tau}$$

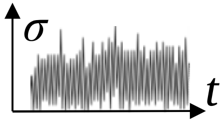

$$n(t) = n_T\left(1 - \exp\left(-\sum_{i=1}^{N}\frac{kT^i}{h}\exp\left(-\frac{U}{kT^i}\right)\int_0^{1/f}\exp\left(\frac{\gamma\sigma^i(\tau)}{kT^i}\right)d\tau\right)\right)$$

Fatigue life predictions CA

- Biaxial case gives shorter fatigue life for a given maximum mechanical bearing stress, $\sigma^b{}_{max}$.
- Biaxial case gives longer fatigue life for a given maximum resultant bearing stress, $\sigma^b{}_{res,max}$.
- Sizing of the biaxially loaded joints, based on $\sigma^b{}_{res,max}$, using uniaxial fatigue data is conservative.

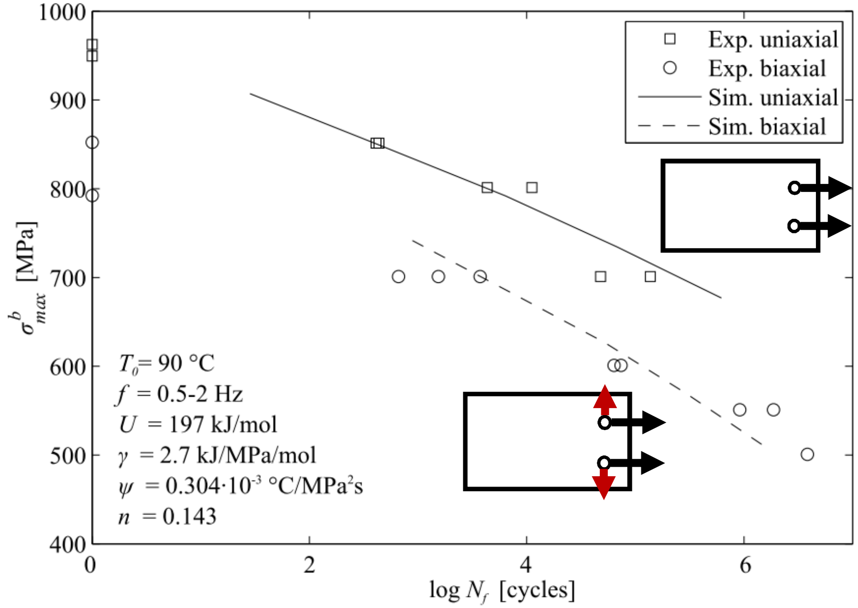

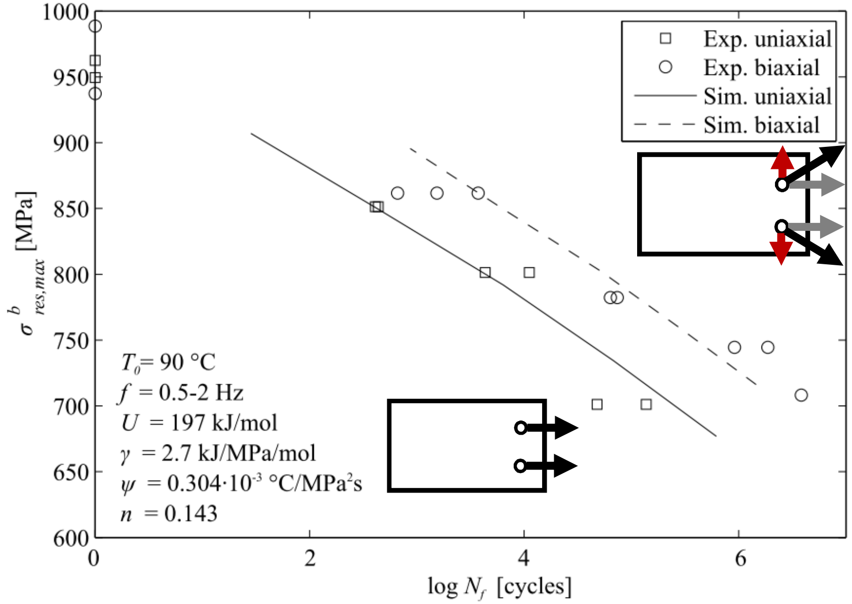

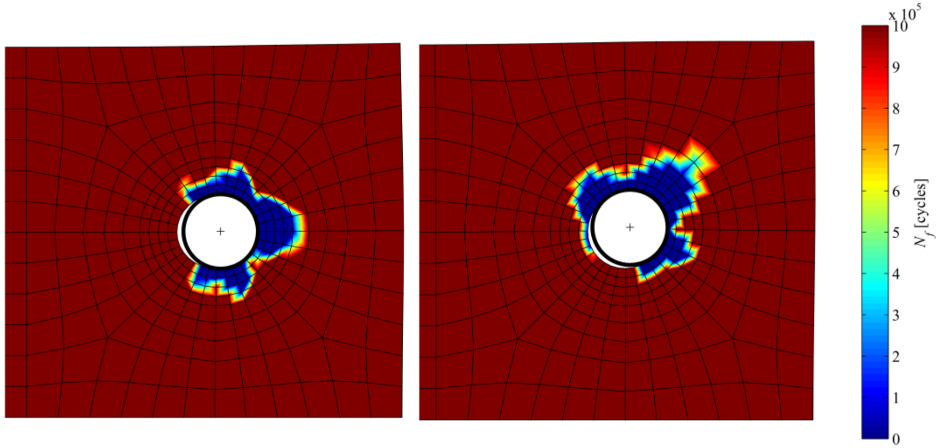

Fatigue life predictions VA

- Same trend is observed in VA loading.
- Larger scatter in VA loading.

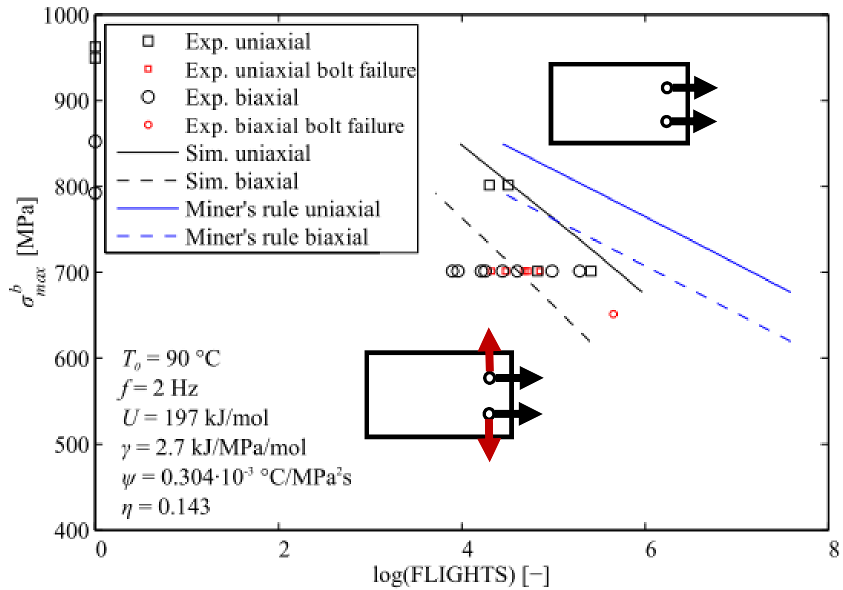

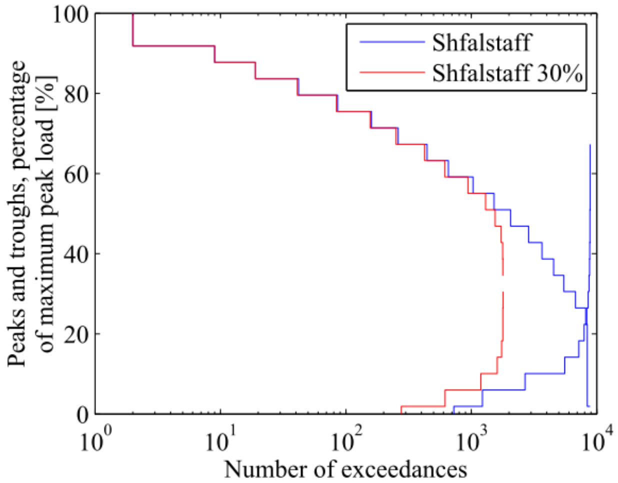

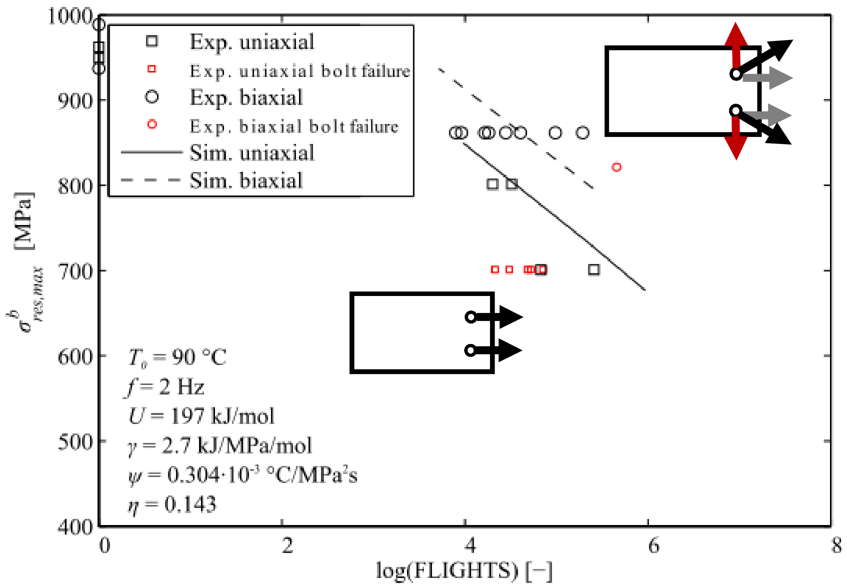

Thank you for your attention !